First-principles study of silicon bulk and nanowire (111) surfaces terminated with trihydrides: Symmetric, rotated, and tilted

Hu Xu,[1,2] Xiaohong Zhang,[2] and R. Q. Zhang[1,*]
[1]*Center of Super-Diamond and Advanced Films (COSDAF) & Department of Physics and Materials Science, City University of Hong Kong, Hong Kong SAR, China*
[2]*Nano-organic Photoelectronic Laboratory, Technical Institute of Physics and Chemistry, Chinese Academy of Sciences, Beijing 100190, China*
(Received 9 April 2009; revised manuscript received 5 July 2009; published 25 August 2009)

We report the structural stability and electronic properties of silicon bulk and nanowire (111) surfaces terminated with symmetric, rotated, and tilted trihydrides based on first-principles calculations. For the bulk surfaces, the one with a tilted trihydride was found to be the most stable with the rotated one next to it in both total-energy calculations and molecular-dynamics simulations. A similar stability trend was further obtained for ⟨110⟩ silicon nanowires. These stability characteristics were shown to be sensitively determined by the surface hydrogen chemical-potential changes. Interestingly, the tilting of the surface trihydride from a symmetric configuration resulted in a noticeable blueshift in the band gap for the Si nanowire, opening up the possibility that the electronic properties can be tuned. The above effects of surface terminations are generic and apply as well to similar materials composed of, for instance, Ge and C, as also demonstrated.

DOI: 10.1103/PhysRevB.80.075428 PACS number(s): 73.22.−f, 61.46.−w, 68.43.Bc

I. INTRODUCTION

Because of its great advantages in the electronics industry, silicon (Si) has become the most important semiconductor material. New interest in Si materials has arisen in the past 20 years owing to the miniaturization of electronic components down to the nanoscale. Si nanostructures are expected to offer novel physical and chemical properties and thus are playing an important role in the new generation of the electronics industry. In particular, one-dimensional Si nanowires (SiNWs) are considered the most promising building blocks for atomic-scale devices because they are compatible with current Si-based technology. Large quantities of SiNWs with different growth directions, such as ⟨110⟩, ⟨111⟩, and ⟨112⟩, have been synthesized successfully by either vapor-liquid-solid (Refs. 1 and 2) or oxide-assisted growth methods.[2–4]

A central issue in Si wafer science and technology is the fabrication of defect free, stable Si surfaces. The (111) and (001) Si wafer surfaces[5–7] are fabricated by hydrogen termination of the dangling bonds on the truncated structure of the Si surfaces by removing the native oxide. In particular, the Si(111) surface can be terminated with hydrogen atoms to form either a monohydride phase represented by Si(111):H (Ref. 8) or a trihydride phase represented by $Si(111):SiH_3$.[9] Interestingly, the $Si(111):SiH_3$ surface prefers adopting a configuration rotated 30° from the symmetric one, according to Pandey *et al.*[9] The science and technology of SiNWs similarly require the ability to fabricate low defect, stable surfaces. Recently, Ma *et al.*[4] reported stable trihydride-terminated SiNWs with diameters of 1.3–7 nm, and they demonstrated a significant quantum-size effect in such sufficiently small SiNWs.

Theoretical investigations of hydrogen-terminated Si surfaces using a multiscale approach have been extensively reported. Using first-principles calculations, Northrup *et al.*[10] obtained atomic structures of hydrogen-terminated Si(100) surfaces with a canted dihydride structure. The Si(111):H surface has been studied employing self-consistent pseudopotentials.[11] The $Si(111):SiH_3$ surface was first reported using ultraviolet photoelectron spectroscopy[9] and the structure of the $Si(111):SiH_3$ surface with a 30° rotation of the trihydride was first theoretically verified using a semiempirical tight-binding model[9] to explain the observation in experiments. But studies on Si nanostructure surfaces are relatively rare. Early in 1996, one of the present authors reported the effects of various surface saturations of Si nanostructures.[12] In 2005, we reported a systematic study of the structures and energetics of hydrogen-terminated SiNW surfaces by performing density-functional tight-binding simulations.[13] Our study included SiNWs with different growth directions, diameters, and cross-section shapes. More recently, the relative stability and electronic properties of the Si(100) surface of SiNWs has been studied using first-principles calculations;[14] the results showed that the canted dihydride is more stable than the symmetric dihydride. In contrast, few theoretical studies have been performed on $Si(111):SiH_3$ surfaces[9] and none on trihydride-terminated SiNWs. Thus, further work on the structural stability and electronic properties of trihydride-terminated surfaces and nanowires are both desirable and needed to provide reliable knowledge of this important material. In contrast to the popular belief that the $Si(111):SiH_3$ surfaces with a 30° rotation of the trihydride are the most stable,[9] our findings in this work indicate that the most stable configurations are the Si bulk and nanowire surfaces with tilted trihydrides, and that the electronic properties of the systems are sensitively affected by the surface hydride geometries.

II. MODELS AND COMPUTATIONAL METHOD

We used a ten-layer slab with each dangling bond terminated by a SiH_3 radical to model the $Si(111):SiH_3$ surface and we enclosed the ⟨110⟩ SiNWs with (111) and (110) facets terminated with monohydrides, trihydrides, and dihy-

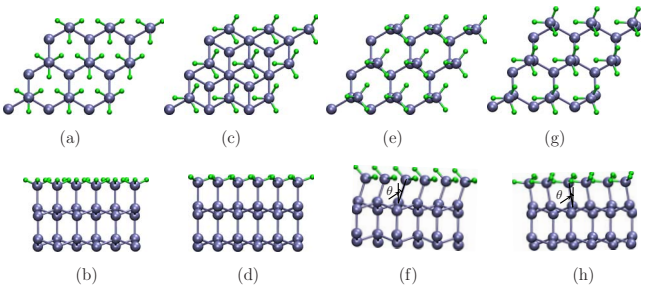

FIG. 1. (Color online) Relaxed structures of Si bulk and nanowire surfaces: (a) top view of the symmetric $Si(111):SiH_3$ surface, (b) side view of the symmetric $Si(111):SiH_3$ surface, (c) top view of the rotated $Si(111):SiH_3$ surface, (d) side view of the rotated $Si(111):SiH_3$ surface, (e) top view of the tilted $Si(111):SiH_3$ surface, (f) side view of the tilted $Si(111):SiH_3$ surface, (g) top view of the trihydride-terminated (111) facet of the nanowire, and (h) side view of the trihydride-terminated (111) facet of the nanowire.

drides. We placed these models in periodic supercells (referred to as (1×1) supercells), respectively. We then performed calculations using density-functional theory (DFT) (Refs. 15 and 16) within the local-density approximation[17] and employed the projected augmented wave method[18] as implemented in the Vienna *ab initio* simulation package (VASP).[19,20] A cut-off energy of 450 eV used throughout the calculations is large enough to ensure that the total energies were all converged. We used the $(8\times8\times1)$ and $(1\times1\times4)$ k-point Monkhorst-Pack[21] samplings for the model calculations of the Si bulk and nanowire surfaces, respectively. We then introduced a vacuum region of 12 Å thick between the neighboring Si slabs or SiNWs to effectively avoid their interactions. We employed the conjugate gradient method to optimize the geometry until the Hellmann-Feynman forces on each atom were smaller than 0.02 eV/Å and the change in total energy was less than 10^{-4} eV per cell. We performed test calculations to make sure that the results using these parameters were fully converged. We further performed molecular-dynamics (MD) simulations based on the same level of DFT to study the $Si(111):SiH_3$ surfaces at a temperature of 300 K.

III. RESULTS AND DISCUSSION

To calculate the Si surfaces using slab models and nanowires, we adopted the optimized lattice parameter for bulk Si (5.403 Å) to construct the initial-model configurations. As shown in Fig. 1(a), the nearest H-H distance (d_2) is 1.563 Å on a surface with the trihydrides in their symmetric configurations. Because the electronegativity of the H atom is 2.1, higher than that of the Si atom (1.8), the negative charge around the H atoms accumulates, leading to a strong repulsive force among the H atoms. Besides the electrostatic repulsion, the H-H steric repulsion on neighboring trihydrides may also play a role in determining the surface structure. The H-H repulsion is the driving force for the rotation of the SiH_3 radical[9] and this repulsion may decrease along with the rotation of the SiH_3 radical from a symmetric configuration. To show such a change, we fixed the rotation angles of the SiH_3

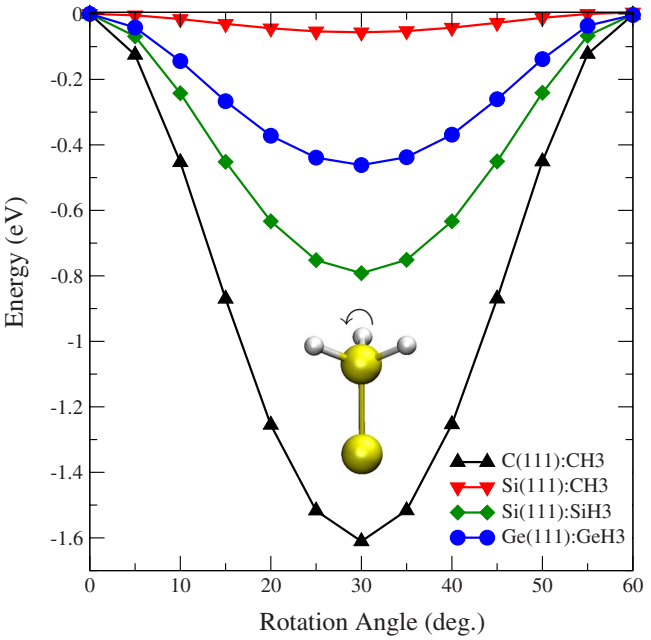

FIG. 2. (Color online) Energy differences relative to symmetric surfaces as a function of rotation angles of XH_3 (X=C, Si, and Ge). All total energies of the symmetric surfaces are set to zero.

radical to certain values between 0 and 60° each with 5° increments; the energy differences between the symmetric and rotated surfaces are plotted in Fig. 2. Obviously, the 30° rotation of the SiH_3 radical results in a stable $Si(111):SiH_3$ surface and the rotated $Si(111):SiH_3$ surface is 0.84 eV lower in energy than that of the symmetric surface. Additionally, the rotated surfaces with angles ranging from 5° to 55° are fully optimized and the SiH_3 radicals spontaneously rotate back to 30.4° because they encounter no energy barrier during the geometrical optimization.

To verify whether the above findings are generic and also present on other semiconductor surfaces, we extended our study to the $C(111):CH_3$, $Si(111):CH_3$, and $Ge(111):GeH_3$ surfaces. We found that these surfaces also adopt a similar 30° rotation caused by the repulsive forces with their energy differences as a function of the rotation angles shown in Fig. 2. Table I lists the structural parameters of the investigated surfaces. As Fig. 2 and Table I show, the energy reduction induced by rotating the trihydrides depends mainly on the d_2 distance of the symmetric surfaces. The H atom of CH_3 radical is almost neutral thus steric repulsion is the major factor driving the rotation. The symmetric $C(111):CH_3$ surface has the strongest repulsion with the shortest d_2 distance so that the total energy is significantly reduced by 1.6 eV along with the 30° rotation of the CH_3 radical. The symmetric $Si(111):CH_3$ surface has the largest d_2 distance among the investigated surfaces, leading to the weakest H-H repulsion.

Besides the d_2 distance, the negative charges of H atoms also play an important role in determining the repulsion force. Since the electronegativity of Si is slightly smaller than that of Ge, the negative charge around H atom of SiH_3 radical is a little more than that of GeH_3 radical. The d_2 distance of the $Si(111):SiH_3$ is 0.05 Å smaller than that in $Ge(111):GeH_3$ surface and the energy gained from the 30°

TABLE I. The optimized H-H distance of the same XH_3 (d_1), the H-H distance of the neighboring XH_3 (d_2), the distance of the topmost X atoms (X-X), the X-H bond length (X-H), and rotation angle (θ) (X=C, Si, and Ge).

Structure		d_1	d_2	X-X	X-H	θ
$Si(111):SiH_3$	symmetric	2.345	1.563	3.907	1.468	0
	rotated	2.420	2.118	3.854	1.489	30.4
$Si(111):CH_3$	symmetric	1.777	2.043	3.820	1.101	0
	rotated	1.788	2.411	3.812	1.103	30.9
$C(111):CH_3$	symmetric	1.508	1.154	2.662	1.025	0
	rotated	1.674	1.442	2.631	1.055	30.2
$Ge(111):GeH_3$	symmetric	2.457	1.612	4.069	1.529	0
	rotated	2.501	2.227	4.024	1.541	30.3

rotation of the SiH_3 radical is 0.3 eV larger than that of the GeH_3 radical. Even the d_2 distance of the $Si(111):GeH_3$ is a bit smaller (about 0.06 Å) than that of the $Si(111):SiH_3$ surface; however, the energy gained due to the 30° rotation of the trihydride for the $Si(111):SiH_3$ is still 0.04 eV larger than that of the $Si(111):GeH_3$ surface. Therefore, the electrostatic repulsion is stronger in the $Si(111):SiH_3$ surface and the $Ge(111):GeH_3$ surface involves a weaker repulsion.

Surprisingly, superior to the trihydride rotation, we found that the trihydride tilting further reduces the repulsion force. While the SiH_3 radical tilting weakens the Si-Si bond energy, it also reduces the repulsive force. The bond-energy reduction and the repulsion decrease thus compete. One hydrogen atom of the SiH_3 radical departs slightly from the surface while the other hydrogen atoms remain close to the surface with the Si-H bond almost parallel to the tilted $Si(111):SiH_3$ surface, as Figs. 1(e) and 1(f) show. The tilting angle θ of the SiH_3 radical is 16°, as labeled in Fig. 1(f). Additional stability is gained with a further increase in the d_2 distances from 1.493 to 1.502 Å, lowering 0.09 eV in the energy of the tilted $Si(111):SiH_3$ surface from that of the rotated surface. Our results show that the surface with tilted trihydrides is the most energetically favorable structure whereas the surface with rotated trihydrides is metastable. To confirm the structural stability of this tilted configuration, we performed further MD simulations starting from the symmetric surface. The time step, temperature, and duration used in the MD simulations were 1 fs, 300 K, and 2 ps, respectively. The MD results are shown in Fig. 3. At the beginning of the MD simulation, the symmetric surface was unstable with high energy; then, the energy decreased rapidly due to rotation and tilting of SiH_3 radicals, leaving mainly thermal vibration of the SiH_3 radicals around the tilting configuration. At 0.5 ps, the $Si(111):SiH_3$ surface involves a 13° tilting angle with two hydrogen atoms of the SiH_3 radical departing slightly from the surface. Interestingly, after 1 ps the structure in the MD simulation result is similar to that of the structure directly optimized which is shown in Fig. 1(f). To verify the validity of the simulation using (1×1) supercell presented above, we also performed MD simulations using (2×2) and (3×3) supercells, respectively. Similar to the case of (1×1) supercell, the SiH_3 radicals favor tilting to one side, along with thermal vibration. The MD simulation results using (2×2) and (3×3) supercells also show that the SiH_3 radical disfavor a randomly tilted configuration because the randomly tilted configuration will result in stronger repulsion force. Using the (1×1) supercell, we also obtained a tilted $Si(111):SiH_3$ surface by MD simulations and the tilting angle of the SiH_3 radical is around 16°. Tilted trihydrides are generic among the investigated surfaces with a strong repulsion. The system energy of the $C(111):CH_3$ surface with the strongest repulsion can be greatly reduced by 0.21 eV and the tilting angle of the trihydrides is 11°. As a result of the weaker repulsion, the total energy of the $Ge(111):GeH_3$ surface with titling trihydrides is slightly reduced by 0.06 eV with a 15° tilted angle. Because of the weakest H-H repulsion, we found no tilted CH_3 radicals on the $Si(111):CH_3$ surface. The $Si(111):CH_3$ surface with a 30° rotation of the CH_3 radical is an energetically favorable structure, which is consistent with other DFT results.[22]

Next, we studied the ⟨110⟩ SiNWs with their facets terminated with monohydride, dihydride, and trihydride. The structures studied here include (a) a ⟨110⟩ wire with four monohydride-terminated (111) facets [Fig. 4(a)]; (b) a ⟨110⟩ wire with four trihydride-terminated (111) facets [Fig. 4(b)];

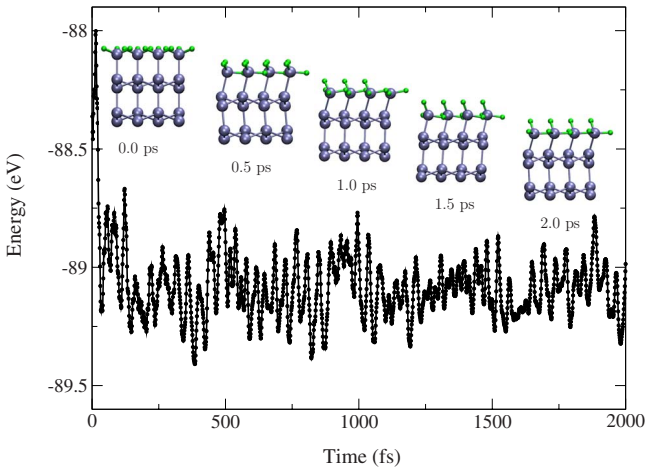

FIG. 3. (Color online) Energies of MD simulation results as a function of time at T=300 K. The snapshots of MD simulation results at 0.0, 0.5, 1.0, 1.5, and 2.0 ps are also shown along with MD simulation time.

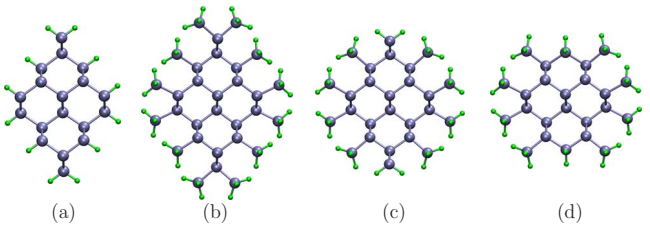

FIG. 4. (Color online) Relaxed top views of ⟨110⟩ SiNWs. (a) Wire A with four monohydride-terminated (111) facets, (b) wire B with four trihydride-terminated (111) facets, (c) wire C with four trihydride-terminated (111) facets and two symmetric dihydride-terminated (100) facets, and (d) wire D with four trihydride-terminated (111) facets and two canted dihydride-terminated (100) facets.

(c) a ⟨110⟩ wire with four trihydride-terminated (111) facets and two symmetric dihydride-terminated (100) facets [Fig. 4(c)]; and (d) a ⟨110⟩ wire with four trihydride-terminated (111) facets and two canted dihydride-terminated (100) facets [Fig. 4(d)]. We optimized both the lattice constant c and the internal coordinates of the SiNWs. The optimized lattice constants along the axis were 3.844, 3.905, 3.891, and 3.911 Å for wires A, B, C, and D, respectively. Because of the H-H repulsion in the trihydride-terminated SiNWs, the lattice constants noticeably increased. The trihydride-terminated (111) facets of the SiNWs have been observed using STM images,[4] which were correlated with the bending stress's weakening of the back bonds of the top-layer Si atoms. Besides the bending stress, we found that the SiH_3 radicals tilting along the growth direction further enhances the stability of these nanowires. As Figs. 1(g) and 1(h) show, the SiH_3 radicals distributed near the edge of the facet involve some bending toward the edge; the SiH_3 radicals also tilt at an angle along the growth direction. The above effects will dramatically increase d_2 distance up to 2.75 Å, leading to a weaker repulsion. The tilted angle θ of the trihydride-terminated wires is around 9°, as labeled in Fig. 1(h), which is smaller than that in the surface terminated with tilted trihydrides. As the diameter of the SiNWs increases, the tilting angle θ approaches 16° on the tilting surface.

To quantitatively evaluate the energetic stability of the surfaces of the silicon bulk and nanowires, we calculated their formation energies according to

$$E_f(\mu_H) = E_{tot} - n_{Si}\mu_{Si} - n_H\mu_H + n_H e_0, \quad (1)$$

where E_{tot} is the total energy of the studied configuration, and n_{Si} (n_H) are the number of Si (H) atoms. e_0 is the zero-point energy arising from the Si-H vibration; μ_{Si} is the chemical potential of Si and is equal to the value in the bulk Si; μ_H is the chemical potential of H, and μ_H can be tuned by changing the temperature and pressure of the H reservoir. High temperature or low pressure lead to low μ_H. For example, at 1300 K (p=1 atm) μ_H is around 1 eV lower than that at T=0 K.[23,24] μ_H^0 is the chemical potential of H in which the formation energy of a SiH_4 molecule formed from a reservoir of H and bulk Si is equal to zero. Thus, μ_H^0 is equal to $(E_{SiH_4}+4e_0-\mu_{Si})/4$. We then considered the μ_H relative to μ_H^0, that is, $\Delta\mu_H=\mu_H-\mu_H^0$.

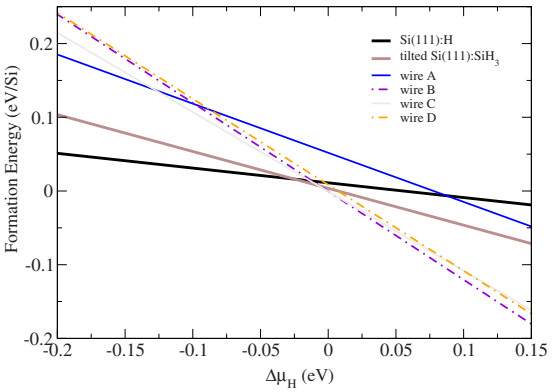

FIG. 5. (Color online) Calculated formation energies for various structures as a function of $\Delta\mu_H$.

The calculated formation energies as a function of $\Delta\mu_H$ are plotted in Fig. 5. The transition in relative stability between the Si(111):H and the tilted Si(111):SiH_3 surfaces occurs when $\Delta\mu_H$ is equal to −0.025 eV. Wire A is the most favorable when $\Delta\mu_H<-0.128$ eV and becomes completely unfavorable when $\Delta\mu_H>-0.087$ eV. Wire B is the most stable until $\Delta\mu_H$ exceeds 0.002 eV but it involves the highest formation energy when $\Delta\mu_H<-0.265$ eV. Wire C is found to be the most stable when $-0.128<\Delta\mu_H<0.002$ eV. But wire D is always unfavorable. We conclude that the energetically favorable structure depends mainly on $\Delta\mu_H$ and a slight change in $\Delta\mu_H$ can significantly affect the configuration. Our results open up the possibility of tuning the structural stability of monohydride- or trihydride-terminated bulk surfaces and nanowire surfaces by controlling the $\Delta\mu_H$.

Fig. 6 shows the band structures of the surfaces of bulk Si and SiNWs. To directly compare the electronic properties between these models, we folded the band structures of the Si(111):SiH_3 surfaces to make them consistent with the SiNWs along the growth direction. The rotated and tilted Si(111):SiH_3 surfaces have respective indirect band gaps of 0.76 and 0.78 eV, a valence-band maximum (VBM) at the Γ point, and a conduction-band minimum (CBM) at around 92% from Γ to A. Because the VBM and CBM are localized in the core of the surfaces, the band gaps are insensitive to the SiH_3 configurations. As the dimensions are reduced from the surface to a one-dimensional nanowire, the quantum confinement will increase the energy of the CBM and decrease the energy of the VBM. Therefore, the SiNWs have larger band gaps than those of the Si surface and are 1.29, 1.43, 1.36, and 1.69 for wires A, B, C, and D, respectively. The

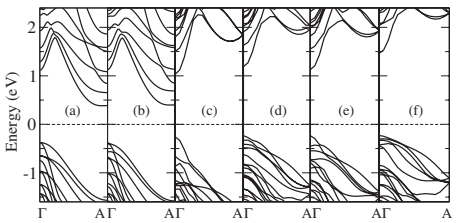

FIG. 6. Band structures of (a) the rotated Si(111):SiH_3 surface, (b) the tilted Si(111):SiH_3 surface, (c) wire A, (d) wire B, (e) wire C, and (f) wire D.

SiNWs also exhibit an indirect to direct band-gap transition for the ⟨110⟩ SiNWs.[14] The SiH_3 radicals have a pronounced influence on the band gap of the wire. For instance, the band gap of wire B is 0.14 eV larger than that of wire A, leading to a blueshift in the band gap. The orientation distribution of dihydride on the (100) facet also obviously influences the band gap of the SiNWs, as the band gap of canted wire D is 0.33 eV larger than that of the symmetric wire C.

IV. CONCLUSIONS

We have evaluated the structural stability and electronic properties of trihydride-terminated silicon bulk surfaces and nanowire surfaces. Using both first-principles calculations and MD simulations, we first revealed the most energetically favorable $Si(111):SiH_3$ surface to be the one terminated with tilted trihydrides. We further obtained the tilted trihydrides for trihydride-terminated SiNWs to be the most favorable. We found similar energetically favorable tilted trihydrides in other IV group semiconductor surface systems, including the $C(111):CH_3$ and $Ge(111):GeH_3$. Structural stability was shown to be sensitive to $\Delta\mu_H$, a slight change in which could obviously alter the stability of these configurations. The band gap of the SiNWs could be tuned by trihydride termination and the orientation distribution of the dihydride, indicating the possibility of tailoring the electronic properties of SiNWs using surface hydrides. The findings are helpful in understanding the structural and electronic properties of trihydride-terminated Si bulk and nanowire surfaces and their uses in device applications.

ACKNOWLEDGMENTS

The work described in this paper is supported by the Research Grants Council of Hong Kong SAR (Project No. CityU 103106), Centre for Applied Computing and Interactive Media (ACIM) of the City University of Hong Kong, and the National Basic Research Program of China (Grant No. 2006CB933000).

*Corresponding author; aprqz@cityu.edu.hk

[1] A. M. Morales and C. M. Lieber, Science **279**, 208 (1998).
[2] Y. F. Zhang, Y. H. Tang, N. Wang, D. P. Yu, C. S. Lee, I. Bello, and S. T. Lee, Appl. Phys. Lett. **72**, 1835 (1998).
[3] R. Q. Zhang, Y. Lifshitz, and S. T. Lee, Adv. Mater. (Weinheim, Ger.) **15**, 635 (2003).
[4] D. D. D. Ma, C. S. Lee, F. C. K. Au, S. Y. Tong, and S. T. Lee, Science **299**, 1874 (2003).
[5] M. Gherasimova, R. Hull, M. C. Reuter, and F. M. Ross, Appl. Phys. Lett. **93**, 023106 (2008).
[6] N. Hirashita, M. Kinoshita, I. Aikawa, and T. Ajioka, Appl. Phys. Lett. **56**, 451 (1990).
[7] Y. Morita and H. Tokumoto, Appl. Phys. Lett. **67**, 2654 (1995).
[8] G. S. Higashi, Y. J. Chabal, G. W. Trucks, and K. Raghavachari, Appl. Phys. Lett. **56**, 656 (1990).
[9] K. C. Pandey, T. Sakurai, and H. D. Hagstrum, Phys. Rev. Lett. **35**, 1728 (1975).
[10] J. E. Northrup, Phys. Rev. B **44**, 1419 (1991).
[11] K. M. Ho, M. L. Cohen, and M. Schlüter, Phys. Rev. B **15**, 3888 (1977).
[12] R. Q. Zhang, J. Costa, and E. Bertran, Phys. Rev. B **53**, 7847 (1996).
[13] R. Q. Zhang, Y. Lifshitz, D. D. D. Ma, Y. L. Zhao, T. Frauenheim, S. T. Lee, and S. Y. Tong, J. Chem. Phys. **123**, 144703 (2005).
[14] T. Vo, A. J. Williamson, and G. Galli, Phys. Rev. B **74**, 045116 (2006).
[15] P. Hohenberg and W. Kohn, Phys. Rev. **136**, B864 (1964).
[16] W. Kohn and L. J. Sham, Phys. Rev. **140**, A1133 (1965).
[17] M. C. Payne, M. P. Teter, D. C. Allan, T. A. Arias, and J. D. Joannopoulos, Rev. Mod. Phys. **64**, 1045 (1992).
[18] P. E. Blöchl, Phys. Rev. B **50**, 17953 (1994).
[19] G. Kresse and D. Joubert, Phys. Rev. B **59**, 1758 (1999).
[20] G. Kresse and J. Furthmüller, Phys. Rev. B **54**, 11169 (1996).
[21] H. J. Monkhorst and J. D. Pack, Phys. Rev. B **13**, 5188 (1976).
[22] M. F. Juarez, F. A. Soria, E. M. Patrito, and P. Paredes-Olivera, J. Phys. Chem. C **112**, 14867 (2008).
[23] C. G. Van de Walle and J. Neugebauer, Phys. Rev. Lett. **88**, 066103 (2002).
[24] H. Xu, W. Fan, A. L. Rosa, R. Q. Zhang, and Th. Frauenheim, Phys. Rev. B **79**, 073402 (2009).